



ELSEVIER

Chemistry & Biology 8 (2001) 17–31

**Chemistry
& Biology**www.elsevier.com/locate/chembiol

Research Paper

Energetic, structural, and antimicrobial analyses of β -lactam side chain recognition by β -lactamases

Emilia Caselli ^{a,b, 1}, Rachel A. Powers ^{a, 1}, Larry C. Blaszczak ^c,
Chyun Yeh Earnest Wu ^c, Fabio Prati ^{b, 2}, Brian K. Shoichet ^{a, *}^aDepartment of Molecular Pharmacology and Biological Chemistry, Northwestern University, 303 East Chicago Avenue, Chicago, IL 60611, USA^bDipartimento di Chimica, Università degli Studi di Modena, Via Campi 183, Modena, Italy^cInfectious Diseases Research, Lilly Research Laboratories, Eli Lilly and Co., Lilly Corporate Center, Indianapolis, IN 46285, USA

Received 18 September 2000; revisions requested 13 October 2000; revisions received 24 October 2000; accepted 30 October 2000

First published online 19 December 2000

Abstract

Background: Penicillins and cephalosporins are among the most widely used and successful antibiotics. The emergence of resistance to these β -lactams, most often through bacterial expression of β -lactamases, threatens public health. To understand how β -lactamases recognize their substrates, it would be helpful to know their binding energies. Unfortunately, these have been difficult to measure because β -lactams form covalent adducts with β -lactamases. This has complicated functional analyses and inhibitor design.

Results: To investigate the contribution to interaction energy of the key amide (R1) side chain of β -lactam antibiotics, eight acylglycineboronic acids that bear the side chains of characteristic penicillins and cephalosporins, as well as four other analogs, were synthesized. These transition-state analogs form reversible adducts with serine β -lactamases. Therefore, binding energies can be calculated directly from K_i values. The K_i values measured span four orders of magnitude against the Group I β -lactamase AmpC and three orders of magnitude against the Group II β -lactamase TEM-1. The acylglycineboronic acids have K_i values as low as 20 nM against AmpC and as low as 390 nM against TEM-1. The inhibitors showed little activity against serine proteases, such as chymotrypsin. R1 side chains characteristic of β -lactam inhibitors

did not have better affinity for AmpC than did side chains characteristic of β -lactam substrates. Two of the inhibitors reversed the resistance of pathogenic bacteria to β -lactams in cell culture. Structures of two inhibitors in their complexes with AmpC were determined by X-ray crystallography to 1.90 Å and 1.75 Å resolution; these structures suggest interactions that are important to the affinity of the inhibitors.

Conclusions: Acylglycineboronic acids allow us to begin to dissect interaction energies between β -lactam side chains and β -lactamases. Surprisingly, there is little correlation between the affinity contributed by R1 side chains and their occurrence in β -lactam inhibitors or β -lactam substrates of serine β -lactamases. Nevertheless, presented in acylglycineboronic acids, these side chains can lead to inhibitors with high affinities and specificities. The structures of their complexes with AmpC give a molecular context to their affinities and may guide the design of anti-resistance compounds in this series. © 2001 Elsevier Science Ltd. All rights reserved.

Keywords: Interaction energy; Transition-state analog; Antibiotic resistance; Structure-based inhibitor design; Drug design

1. Introduction

β -Lactamases catalyze the hydrolysis of β -lactam antibiotics, such as penicillins and cephalosporins, and are the

most widespread bacterial resistance mechanism to these drugs [1]. Partly in response to the emergence and spread of β -lactamases, many β -lactam derivatives have been developed; over 40 are currently used in clinical practice. These analogs preserve the β -lactam core of the drug but explore diverse functionality off the C6(7) position of the penicillin/cephalosporin ring, in what we will refer to as the R1 side chain (Fig. 1). The different R1 side chains confer different pharmacological profiles, different bacterial spectra of action, and different levels of resistance to β -lactamases. Whereas early penicillins and cephalosporins,

¹ These authors contributed equally to this paper.

² Also corresponding author. E-mail: fprati@pascal.unimo.it

* Correspondence: Brian K. Shoichet;
E-mail: b-shoichet@northwestern.edu

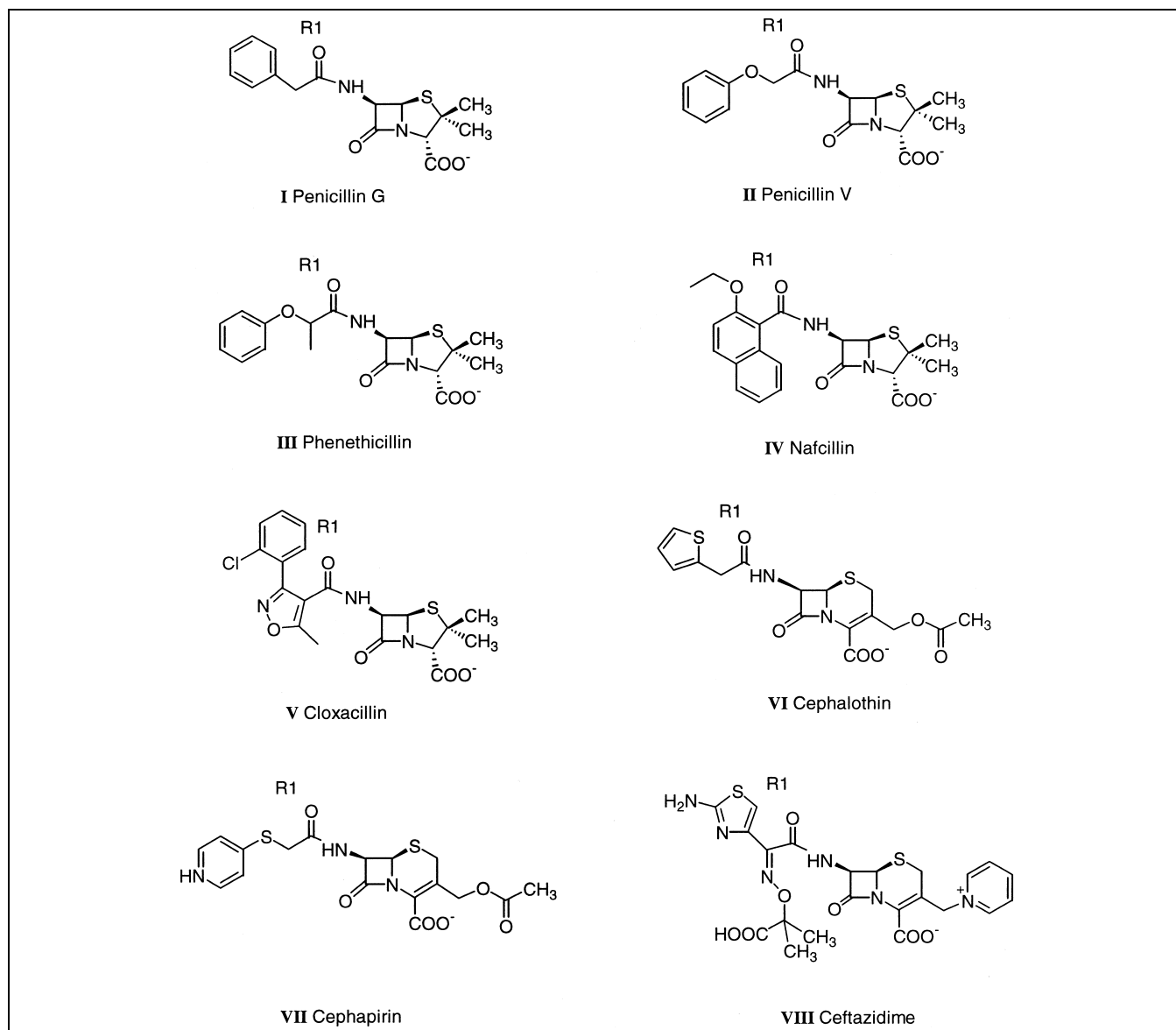
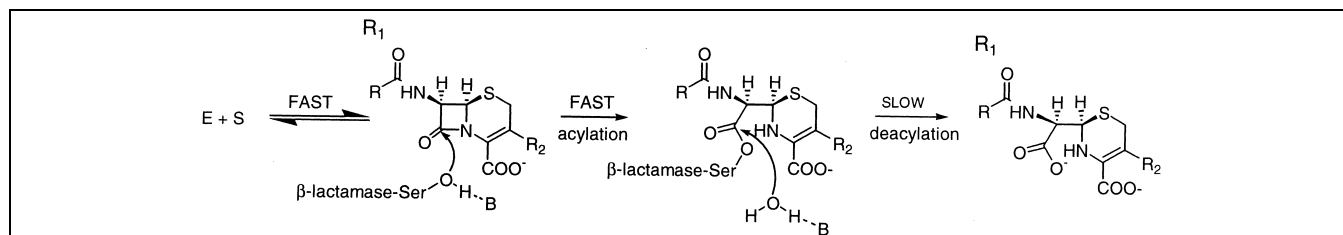


Fig. 1. Clinically used penicillins (I–V) and cephalosporins (VI–VIII)

such as penicillin G and cephalothin (Fig. 1), are rapidly inactivated by β -lactamases, later agents, such as cloxacillin and ceftazidime, are relatively inert to, or indeed inhibit, these enzymes. Despite intense study, it has been difficult to understand how these seemingly defining R1 side chains contribute to β -lactam– β -lactamase recognition.

The problem lies in the covalent bond that β -lactams form with Group I and Group II β -lactamases. In these enzymes, the catalytic serine attacks the lactam bond to form an acyl-adduct (Fig. 2); this step is rapid for β -lactamases. The acyl-adduct is then hydrolyzed in a second step; deacylation is rate determining for Group I β -lac-

Fig. 2. β -Lactam hydrolysis by serine β -lactamases. The deacylation step is slow for β -lactam inhibitors and poor substrates. B represents the general base in the mechanism.

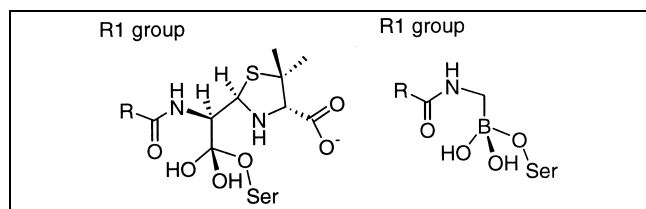
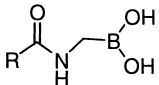
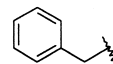
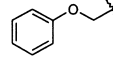
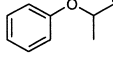
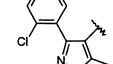
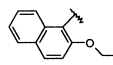

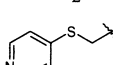
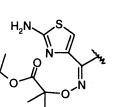
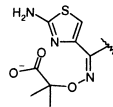
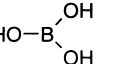
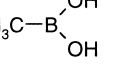


Fig. 3. Comparison between the deacylation high-energy intermediate of a penicillin in a serine β -lactamase and the transition-state analog formed by an acylglycineboronic acid and the same enzyme.

tamases and for poor substrates and inhibitors of both classes of enzyme. The covalent nature of the acyl-adduct, and its rapid formation, means that binding is effectively irreversible; binding equilibria are not readily available through steady state kinetics [2]. This precludes easy energetic analyses, which assume reversible equilibria. In β -lactamases, K_m values are convolutions of irreversible acylation and deacylation rates with reversible on and off rates, and IC_{50} values are often dominated by rates

Table 1
 K_i (μ M) values of acylglycineboronic acids against AmpC and TEM-1

					
compound	β -lactam analog	side chain	K_i (μ M) vs TEM-1	K_i (μ M) vs AmpC	$\Delta\Delta G^b$ from 5 (kcal/mol)
3	---	-H	38	4.8	0.80
5	---	-CH ₃	162	18.5	0.00
6	penicillin G		13.8	0.57	2.06
7	penicillin V		NM ^a	0.70	1.94
8	phenethicillin		NM	0.30	2.44
9	cloxacillin		6.8	0.150	2.85
10	nafcillin		NM	0.033	3.75
11	cephalothin		6.5	0.32	2.40
12	---	-CH ₂ Cl	NM	0.24	2.57
13	cephapirin		NM	0.175	2.76
14	---		NM	0.070	3.30
15	ceftazidime		0.39	0.020	4.04
boronic acids with no amide side chain			K_i (μ M) vs TEM-1	K_i (μ M) vs AmpC	
	Boric acid		1,500	2,800	-2.97
	Methylboronic acid		2,500	1,000	-2.36

Compounds **6** to **10** bear side chains common to the penicillins; compounds **11** to **14** bear side chains common to the cephalosporins. **7** is common to other β -lactams: cefoxitin, nitrocef, and cephaloridine. ^aNot measured. ^bDifferential free energy of binding relative to compound **5** at 298 K. Positive values indicate improved affinity.

Table 2
Selectivity of **3** and **15** for AmpC and TEM-1 β -lactamases versus serine proteases

Enzyme	IC ₅₀ (μ M) for 3	IC ₅₀ (μ M) for 15
AmpC	17	0.081
TEM-1	247	2.4
α -Chymotrypsin	> 2000 ^b	2 000
β -Trypsin	> 400 ^a	> 400 ^a
Elastase	> 400 ^a	450

^aNo inhibition was observed at 100 μ M. The IC₅₀ values assume that inhibition was no greater than 20% at this concentration.

^bNo inhibition was observed at 500 μ M. The IC₅₀ values assume that inhibition was no greater than 20% at this concentration.

of deacylation. Rarely do they reflect binding energies or inhibitor–enzyme complementarity in any simple way [3,4]. Indeed, both structural [5,6] and stability [7] studies have suggested that some β -lactam inhibitors of β -lactamases fit the enzyme poorly – their inhibitory properties derive entirely from their ability to form an acyl-adduct and then block attack by the hydrolytic water. On the other hand, some R1 side chains undoubtedly fit the enzymes well. Identifying, far less quantifying, which ones do so has been difficult.

To investigate the energetic bases of β -lactam functional group recognition by β -lactamases, we have synthesized acylglycineboronic acids that bear the R1 side chains of eight characteristic penicillins and cephalosporins (Fig. 1). Boronic acids are transition-state analog inhibitors of Group I and Group II β -lactamases [8–14] (Fig. 3). Unlike β -lactams, they form reversible adducts with these enzymes; binding energies thus can be calculated directly from K_i values. By comparing the affinities of different

acylglycineboronic acids, we can determine what the different R1 side chains contribute to binding to a β -lactamase. By comparing the affinities to a Group I β -lactamase, AmpC, and a Group II β -lactamase, TEM-1, we can investigate differential recognition between characteristic representatives of the two most widespread classes of β -lactamases. To give the binding energies a molecular context, we have determined the structures of two of these inhibitors in their complexes with AmpC β -lactamase by X-ray crystallography. Comparing one of these structures with that of its β -lactam counterpart in complex with AmpC [6] allows us to investigate how interactions with the R1 side chain differ between the acylated ground state and the presumptive deacylation high-energy intermediate. To explore the application of acylglycineboronic acids to reversing β -lactamase-mediated resistance at the level of cell culture, we have investigated their ability to act synergistically with β -lactams against resistant, pathogenic bacteria.

2. Results

2.1. Synthesis

Six acylglycineboronic acids (**6**, **7**, **8**, **9**, **10**, **11**, **12**) were synthesized through nitrogen displacement with LiN[Si(CH₃)₃]₂ on chloromethylboronic acid pinacol ester **1**, followed by deprotection with equimolar methanol, and finally condensation with an acylchloride. The yield of these two-step syntheses varied from 62 to 92%. Slight changes to this general scheme were performed to synthesize **5**, **13**, and **15**. Deprotection of **4** was performed with

Table 3
Data collection and refinement statistics

	9/AmpC complex	11/AmpC complex
Cell constants (\AA ; $^\circ$)	$a = 118.36$ $b = 77.57$ $c = 97.46$; $\beta = 116.18$	$a = 118.11$ $b = 77.83$ $c = 97.32$; $\beta = 115.83$
Resolution (\AA)	1.75	1.90
Unique reflections	79 142	58 505
Total reflections	287 631	176 832
R_{merge} (%)	6.4 (13.9) ^a	6.3 (17.2) ^a
Completeness (%)	98.6 (94.6) ^a	93.6 (94.5) ^a
$\langle I \rangle / \langle \sigma_I \rangle$	12.9	14.2
Resolution range for refinement (\AA)	20–1.75 (1.79–1.75 \AA) ^a	20–1.90 (1.94–1.90 \AA) ^a
Number of protein residues	716	716
Number of water molecules	499	415
RMSD bond lengths (\AA)	0.014	0.013
RMSD bond angles ($^\circ$)	1.781	1.719
R -factor (%)	19.6	19.4
R_{free} (%)	21.8 ^b	22.7 ^b
Average B -factor, protein atoms (\AA^2)	30.0 ^c	32.0 ^c
Average B -factor, protein atoms (\AA^2 , monomer 1 only)	29.9	31.8
Average B -factor, inhibitor atoms (\AA^2)	40.6 ^c	41.0 ^c
Average B -factor, inhibitor atoms (\AA^2 , monomer 1 only)	36.8	39.9

^aValues in parentheses are for the highest resolution shell used in refinement.

^b R_{free} was calculated with 10% of reflections set aside randomly.

^cValues cited were calculated for both molecules in the asymmetric unit.

acetic acid; reaction with acetic anhydride gave **5** in 60% yield. The condensation of compound **12** with 4-mercapto-pyridine gave **13** in 90% yield. Compound **14** was obtained by preactivating (*Z*)-2-amino- α -[1-(*tert*-butoxycarbonyl)-1-methylethoxyimino]-4-thiazoleacetic acid as a mixed anhydride followed by reaction with the deprotected **4**. The *tert*-butoxycarbonyl group of **14** was removed with TFA to give **15** in 64% yield over three steps. This general synthetic scheme seems well suited to attaching the R1 side chains of β -lactams to glycineboronic acids.

2.2. Binding constants

The differential affinities of the acylglycineboronic acids allowed us to determine the contributions of the R1 side chain of β -lactams to molecular recognition by the various enzymes. Against the Group I β -lactamase AmpC, the K_i

values spanned a 1000-fold range, from 20 nM to 19 μ M (Table 1). Comparing the minimal amide side chain of **3** (K_i 4.8 μ M) to methylboronic acid (K_i 1 mM) or to boric acid (K_i 2.8 mM) suggests that the amide group itself contributes 3.2 kcal/mol to binding in this series (using $\Delta\Delta G_{\text{bind}} = -RT\ln K_1/K_2$). Comparing the affinity of **3** to compounds with more elaborate side chains, such as the ceftazidime analog **15** (K_i 20 nM), suggests that variations distal to the amide group can contribute at least 4.0 kcal/mol further to the interaction energy with AmpC.

The acylglycineboronic acids bound less tightly to the Group II β -lactamase TEM-1 than they did to AmpC (Table 1). Against TEM-1, K_i values varied from 0.39 to 162 μ M. These values were 8–40-fold worse (higher) than with AmpC. As with AmpC, compound **15**, bearing the ceftazidime side chain, was the most active compound against TEM-1 (K_i 0.39 μ M).

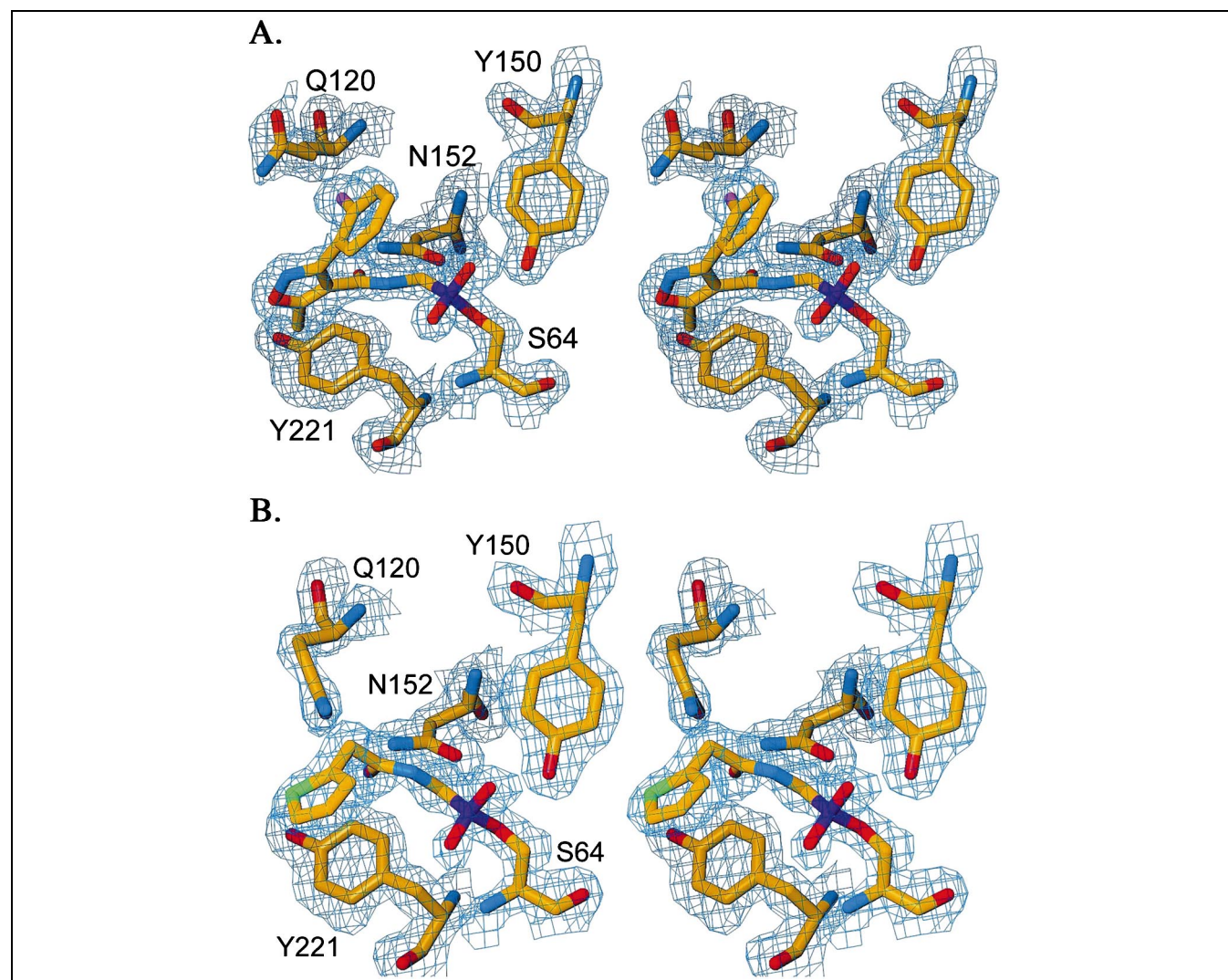


Fig. 4. Stereoview of $2F_o - F_c$ electron density of the refined models for AmpC complexes of (A) compound **9** and (B) compound **11**. The density is contoured at 1 σ . Carbon atoms are colored orange, oxygen atoms red, nitrogen atoms blue, sulfur atoms green, chlorine atoms magenta, and boron atoms purple. These figures were generated using Turbo [38].

2.3. Selectivity testing

Compound **3**, bearing the minimal amide side chain, and compound **15**, bearing the relatively elaborate ceftazidime side chain, were tested for β -lactamase selectivity versus the serine proteases α -chymotrypsin, β -trypsin, and elastase (Table 2). Compound **3** showed no activity up to 100 μ M against any of the proteases. Compound **15** had an IC_{50} of 82 nM for AmpC and a projected IC_{50} of 2 mM for α -chymotrypsin, 450 μ M for elastase, and no measurable activity against β -trypsin. These assays were performed at a similar ratio of substrate concentration to K_m for each enzyme.

2.4. X-ray crystallographic structure determination

The structures of both **9** and **11** in complex with the Group I β -lactamase AmpC were determined to 1.75 Å and 1.90 Å resolution, respectively (Table 3). The location of the inhibitor in each complex was unambiguously identified in the initial $F_o - F_c$ difference maps when contoured at a level of 3 σ . Simulated annealing omit maps of the refined models agree well with the placement of the inhibitors in the active sites (not shown).

The quality of each of the models was analyzed with the program Procheck [15]. For the model of the complex of **9** with AmpC, 92.9% of the non-proline, non-glycine resi-

Table 4
Interactions in complexed and native AmpC β -lactamase

Interaction	9/AmpC ^a	11/AmpC ^a	Native ^b
S64N-O1	2.8	3.0	NP ^c
A318N-O1	2.8	2.8	NP
A318O-O1	2.7	2.8	NP
Y150OH-O2	2.6	2.6	NP
Wat402-O2	2.9	2.9	NP
Y150OH-K315N ζ	3.0	2.9	2.5
Y150OH-S64O γ	2.9	2.8	3.2
Y150OH-K67N ζ	3.4	3.4	3.1
K67N ζ -A220O	2.9	2.8	3.5
K67N ζ -S64O γ	2.7	2.7	3.5
Wat402-T316O γ 1	2.9	2.9	3.8 ^d
Wat402-Wat403	2.7	2.9	NP
Wat403-N346O δ 1	2.7	2.6	NP
Wat403-R349N η 1	3.1	3.0	NP
A318O-N4	3.3	4.3	NP
N152N δ 2-O6	2.5	2.8	NP
Q120N ϵ 2-O6	5.2	2.9	NP
N152O δ 1-K67N ζ	2.7	2.6	2.7
N152N δ 2-Q120O ϵ 1	6.6	2.7	3.0
Wat569-O10	3.1	NP	NP
Wat867-O6	2.9	NP	NP

^aDistances are for monomer 1 of the asymmetric unit. Monomer 1 was chosen because electron density for the inhibitors was better and average B -factors for the inhibitor atoms were 3–8 Å² lower in monomer 1 versus monomer 2; the respective distances differ only slightly between the two monomers. The RMSD for the C α atoms of the two monomers is 0.22 Å for **9**/AmpC and 0.23 Å for **11**/AmpC. The RMSD for the inhibitor atoms between the two molecules is 0.204 Å for **9**/AmpC and 0.271 Å for **11**/AmpC when the C α atoms are overlaid. ^bDistances are for monomer 2 of the asymmetric unit. ^cNot present. ^dIn the native structure, Wat402 is called Wat387.

dues were in the most favored region of the Ramachandran plot (7.1% in the additionally allowed region), and for the complex of **11** with AmpC, 91.9% of the non-proline, non-glycine residues were in the most favored region (8.1% in the additionally allowed region). The structures have been deposited with the PDB as 1FSY (complex with **9**) and 1FSW (complex with **11**).

In both structures electron density is observed connecting O γ of the catalytic Ser64 to the boron atom of the inhibitors (Fig. 4). The geometry around the boron is tetrahedral, as expected. The O1 of the boronic acid is within good hydrogen-bonding distance of the backbone nitrogens of Ser64 and Ala318 and also the backbone oxygen of Ala318 (Table 4). These interactions are highly conserved in β -lactamase structures with transition-state analogs [10,12–14,16]. The O2 of the boronic acid, which probably represents the position of the deacylating water in the high-energy intermediate [6,13], hydrogen bonds with the putative catalytic base Tyr150 [16,17] (Table 4). Two well-ordered water molecules are also observed in the region of the tetrahedral center of each complex, as seen in a previous structure of AmpC in complex with a boronic acid inhibitor [13]. The first water (Wat402) interacts with O2 of the boronic acid, O γ 1 of Thr316, and another water molecule (Wat506). The second water (Wat403) interacts with Wat402, as well as with O δ 1 of Asn346 and N η 1 of Arg349. In the complex with **9**, Wat403 is also within hydrogen bonding distance to another water molecule (Wat549) (Table 4).

In the crystal structures, the amide groups in the acylglycineboronic acids are placed close to where the analogous R1 side chain amide is placed in the structures of complexes between β -lactams and β -lactamases [6,18,19]. The amide groups in both the transition-state analog structures and the β -lactam acyl-adducts make similar interactions with the enzymes. In the structure of **11** with AmpC, the carbonyl oxygen (O6) of the amide group interacts with N δ 2 of Asn152 (2.8 Å) and N ϵ 2 of Gln120 (2.9 Å) (Table 4); both residues are completely conserved among Group I β -lactamases. In the complex of **9** with AmpC, only the interaction between N δ 2 of Asn152 and O6 is seen (2.5 Å). Gln120 appears unable to hydrogen bond with O6 due to a steric conflict that would occur with the chlorine atom of the inhibitor; instead, this residue has rotated by 119° around χ^2 , away from the chlorine atom. In the complex with **9**, an interaction is also observed between Ala318O and N4 (3.3 Å) (Table 4).

The unique part of the R1 side chain of compound **11**, the thiophene ring, appears to make few interactions with AmpC. Difference density suggests that this ring can assume two conformations, which differ from each other by a 180° rotation around the C7–C8 bond. In each of the conformations, the atoms to which the thiophene is nearest are Thr319C and Asn343N δ 2; the distances are between 3.4 and 3.5 Å. The nearest atom to the sulfur of the thiophene ring in one conformation is the C β of Ala318 (3.7 Å); there is also a water molecule (Wat745) 3.4 Å away from the sulfur in this conformation. In the

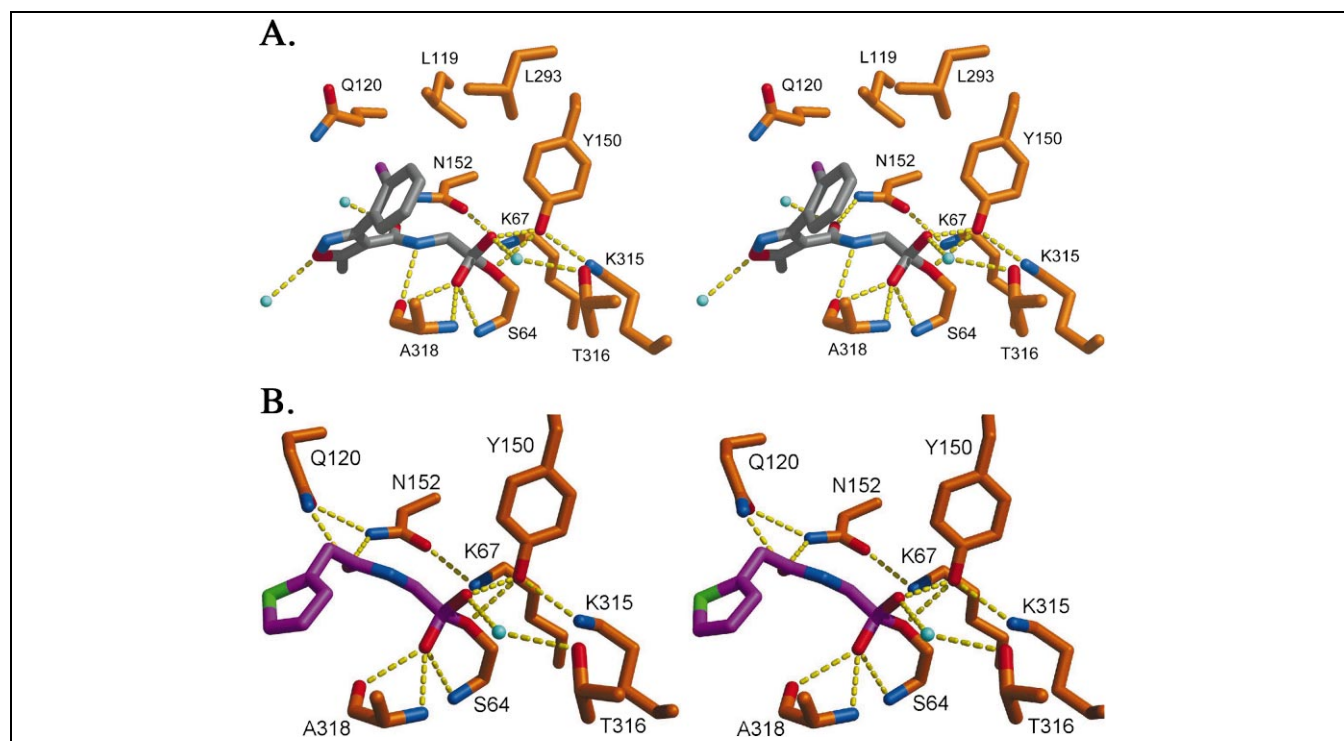


Fig. 5. Key polar interactions observed between AmpC and (A) compound **9** and (B) compound **11**. Dashed yellow lines indicate hydrogen bonds. Atoms are colored as in Fig. 4, except for the inhibitors where carbon atoms are colored gray in **9** and magenta in **11**. Cyan spheres represent water molecules. Interaction distances are listed in Table 4. These figures were generated with MidasPlus [39].

Table 5
Synergy of compounds **10** and **15** with β -lactams against β -lactamase-producing bacteria

<i>E. cloacae</i> 265A				<i>S. aureus</i> V41			
Cefotaxime MIC ^a ($\mu\text{g/ml}$)	10 ($\mu\text{g/ml}$)	Cefotaxime MIC ^a ($\mu\text{g/ml}$)	15 ($\mu\text{g/ml}$)	Amoxicillin MIC ^a ($\mu\text{g/ml}$)	10 ($\mu\text{g/ml}$)	Amoxicillin MIC ^a ($\mu\text{g/ml}$)	15 ($\mu\text{g/ml}$)
128	0	128	0	64	0	64	0
64	2	64	2	64	2	64	2
64	4	64	4	32	4	64	4
64	8	16	8	32	8	32	8
32	16	2	16	16	16	32	16
16	32	1	32	8	32	32	32
8	64	0.5	64	2	64	16	64
4	128	0.5	128	0	128	8	128

^aThe MIC of the β -lactam, either cefotaxime or amoxicillin, in the presence of the adjacent concentration of inhibitor.

second conformation, the sulfur is nearest to N ϵ 2 of Gln120 (4.3 Å) and is close to two water molecules (Wat744, 3.8 Å and Wat743, 3.9 Å).

In the complex of **9** with AmpC, O10 of the isoxazole ring interacts with a water molecule (Wat569, 3.1 Å). The exocyclic methyl group (C9) packs against the aryl ring of Tyr221. The chlorobenzyl ring of the inhibitor is located in a hydrophobic pocket formed by residues Leu119 and Leu293. The C β of Ala318 also contributes to burial of this ring. The distances range from 3.6 Å (from C18 to C β of Ala318) to 4.3 Å (from C15 to C δ 2 of Leu119 and to C δ 1 of Leu293). This ring is also near residues Asn289 and Asn343 and appears to make van der Waals interactions with these residues. As mentioned above, the chlorine atom is placed near Gln120 (3.8 Å).

2.5. Microbiology

The minimum inhibitory concentration (MIC) of ceftazidime and cefotaxime against the EB5 strain of *Enterobacter cloacae*, which does not produce a Group I β -lactamase, were 0.4 $\mu\text{g/ml}$ and 0.25 $\mu\text{g/ml}$, respectively. Administered alone, neither **10** nor **15** had measurable activity; additionally there was no synergy observed against this strain when these compounds were administered with either ceftazidime or cefotaxime. Similarly, compound **15** had no activity by itself against *Staphylococcus aureus* strain V41; the MIC of compound **10** alone was 128 $\mu\text{g/ml}$ against this strain. Against strain 265A of *E. cloacae*, which hyper-produces a Group I β -lactamase, the MIC values of ceftazidime and cefotaxime rose to 256 and 128 $\mu\text{g/ml}$, respectively. Both compounds **10** and **15** showed synergy with these β -lactams against this strain. Compound **15** reduced the MIC of ceftazidime by 256-fold at 32 $\mu\text{g/ml}$ of the inhibitor (data not shown) and reduced the MIC of cefotaxime by 128-fold at the same concentration (Table 5). Both inhibitors also showed synergy with amoxicillin against *S. aureus* expressing a Group II β -lactamase (Table 5).

Disk diffusion plate assays were performed to study the effects of compounds **10** and **15** on the efficacy of the

β -lactam ceftazidime. As expected, the plate containing *E. cloacae* that does not produce a β -lactamase shows a large inhibition halo surrounding the upper disks that contain ceftazidime. The lower disks, which contain compound **10** (right) or **15** (left), have no effect on the inhibition halo of ceftazidime, nor do they show any inhibition halos of their own (Fig. 6A). The plate containing *E. cloacae* that hyper-produce a Group I β -lactamase shows greatly reduced inhibition halos surrounding the upper disks containing ceftazidime, and in contrast to the pre-

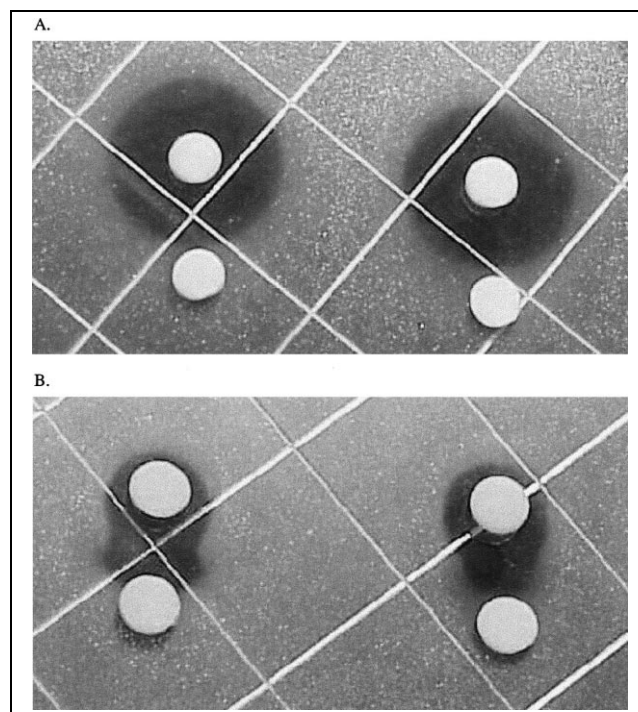


Fig. 6. Synergistic effects of compounds **15** and **10** observed with the β -lactam ceftazidime. (A) *E. cloacae* strain EB5 (β -lactamase negative). Each of the upper disks contains 25 μg ceftazidime. The lower disk on the left contains 100 μg compound **15**, and the lower disk on the right contains 100 μg compound **10**. (B) *E. cloacae* strain 265A (Group I β -lactamase hyper-producer). Each of the upper disks contains 50 μg ceftazidime. The lower disk on the left contains 100 μg of **15**, and the lower disk on the right contains 100 μg of **10**.

vious plate, the inhibition halos in the regions between the two disks are substantially increased (Fig. 6B). This increase in the size of the inhibition halos between the two disks indicates that each compound has a synergistic effect when coupled with ceftazidime.

3. Discussion

The acylglycineboronic acids span five orders of magnitude in affinity for AmpC, from a dissociation constant of 2.8 mM for boric acid itself to 20 nM for the ceftazidime analog **15** (Table 1). This suggests that the R1 side chains of β -lactams can make considerable contributions to affinity for β -lactamases. The result is unexpected, if only because the effect of R1 side chains on affinity has previously been largely unknown. The compounds appear to be selective for β -lactamases, especially Group I β -lactamases resembling AmpC, showing little affinity for serine proteases that are known to be inhibited by peptide boronic acids [20] (Table 2). This is consistent with the specific recognition of the R1 side chains by serine β -lactamases. The differential energies between compounds allow us to interpret the interactions that we observe in the crystal structures of two of these inhibitors, and by analogy, those observed in other β -lactam complexes. Additionally, comparing the X-ray crystal structure of a transition-state analog complex with that of an acyl-enzyme intermediate suggests how recognition of the R1 side chain changes between the transition state and the acylated ground state in Group I β -lactamases.

An important contribution to affinity comes from the amide group common to all the inhibitors. Comparing compound **3** to methylboronic acid suggests that this amide contributes 3.2 kcal/mol to the free energy of binding. This group represents the C6(7) R1 amide that is ubiquitous among β -lactam antibiotics (Fig. 1). In previous structures with β -lactams, the amide oxygen of the side chain has been observed to hydrogen bond to the side chain of the conserved Asn152 (Asn132 in Group II β -lactamases). The amide nitrogen of the R1 side chain has been observed to hydrogen bond to the main chain carbonyl of residue 318 in Group I β -lactamases (residue 237 in Group II β -lactamases) [6,16,18,19,21]. In the X-ray crystal structures of **9** and **11** in complex with AmpC, the R1 amide hydrogen bonds to Asn152 (Fig. 5, Table 4). The hydrogen bonding interaction with Ala318 is observed in the structure of AmpC with **9** but not with **11**. The hydrogen bond between the ligand amide nitrogen and the backbone carbonyl of residue 318/237 may not be as well conserved structurally as that of Asn152/Asn132 with the ligand amide oxygen [6,10].

The distal parts of the R1 side chain, which have been the principle focus of design and modification of semisynthetic β -lactam antibiotics, also contribute to binding affinity. Dissociation constants vary from 700 nM for **7**,

which bears the penicillin V side chain, to 20 nM for **15**, which bears the ceftazidime side chain (Table 1). By comparison to the acetamido side chain in compound **5** (K_i 18 μ M), the contribution to affinity for each group can be determined. For instance, the ceftazidime side chain contributes 4.0 kcal/mol in differential affinity compared to **5**. Intriguingly, β -lactam side chains that are associated with inhibitors of AmpC do not necessarily have higher affinities than boronic acids bearing substrate side chains. For instance, cloxacillin is an inhibitor of AmpC, whereas ceftazidime is a substrate for the enzyme, albeit a poor one; nevertheless, the ceftazidime analog **15** binds 10-fold better to the enzyme than does the cloxacillin analog **9**. Similarly, compound **11**, which bears the side chain of the very good substrate cephalothin, binds only two-fold less well than the cloxacillin analog **9**.

Although Group I and Group II β -lactamases are mechanistically related, the two enzyme groups have different substrate preferences and inhibitor profiles. To investigate differential recognition between these two classes of β -lactamases, the affinity of several of the acylglycineboronic acid inhibitors was determined for the characteristic Group II β -lactamase, TEM-1. Overall, there is a monotonic relationship between the affinity of acylglycineboronic acids for AmpC and for TEM-1, with the affinities for TEM-1 being 8–40-fold worse. TEM-1, traditionally known as a penicillinase, does not appear to be more selective for R1 side chains associated with penicillins than does the cephalosporinase AmpC for the side chains of R1 side chains associated with cephalosporins (Table 1). To the extent that Group I and Group II β -lactamases are selective for cephalosporins and penicillins [3], respectively, this does not seem to owe to differences in the R1 side chains associated with each of these classes of drugs.

The greater affinity of the acylglycineboronic acids for AmpC versus TEM-1 suggests that the R1 side chain contributes more to recognition in Group I β -lactamases than it does in Group II β -lactamases. This suggestion is consistent with residue substitution and inhibition studies in these enzymes. Whereas the R1-amide recognition residue Asn132 of Group II β -lactamases can be substituted with an aspartate or a serine with little loss of enzyme activity [22], the analogous N152D AmpC mutant enzyme loses four orders of magnitude of activity [23]. Also, the C3(4) carboxylate, on the other side of the β -lactam ring, contributes strongly to recognition of β -lactams by Group II β -lactamases but not to Group I β -lactamases [24]. The importance of this carboxylate for Group II β -lactamases is reinforced by a comparison of the activity against TEM-1 of compound **6** with that of an analogous boronic acid, (1R)-1-phenylacetamido-2-(3-carboxyphenyl)-ethylboronic acid. The latter compound has the same R1 side chain as **6** but also has a carboxylate resembling the C3 carboxylate in penicillins [14]. The carboxylate-containing boronic acid has a K_i of 5.9 nM against TEM-1, whereas compound **6** has a K_i of 13.8 μ M.

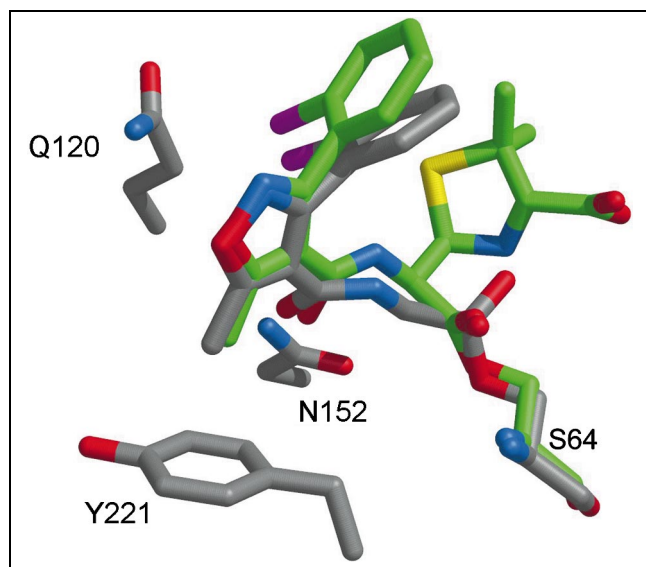


Fig. 7. Overlay of the structure of cloxacillin in complex with the AmpC mutant enzyme Q120L/Y150E and of the transition-state analog **9** in complex with wild type AmpC. Carbon atoms of cloxacillin are colored green, and carbon atoms of **9** are colored gray.

Boronic acids mimic the tetrahedral geometry of the transition state of Group I β -lactamases [6,13,25], and it is interesting to compare their placement of the R1 side chains with that of the β -lactam acyl-adduct structures. When we overlap the structure of the AmpC/**9** complex with that of a mutant AmpC (Q120L/Y150E) bound to cloxacillin [6] in an acyl-adduct, we observe that the two R1 side chains are placed similarly in both structures (Fig. 7). The RMSD between the two side chains is 0.9 Å, and most of the interactions are maintained. The greatest positional differences are at the amide nitrogen at the beginning of the R1 side chain, but even here the transition-state analog and the acyl-adduct maintain the same interactions. On the part of the enzyme, there is little reorganization in the active site region. The RMSD between the C α atoms of conserved residues in the active sites (Ser64, Lys67, residue 150, Asn152, Tyr221, Lys315, and Ala318) of transition-state structure and the acyl-enzyme structure is 0.17 Å (0.44 Å for all atoms of the above residues except residue 150, whose identity differs between the mutant and wild type enzymes). We make two inferences based on this comparison. First, at least for the cloxacillin group, the presence of rest of the β -lactam has little effect on the positioning of the R1 side chain. Second, the similarity of the acyl-adduct ground state to the transition-state analog suggests that progress along the reaction requires little reorganization in the R1 side chain or in the residues with which it interacts. There may be little differential stabilization between the acylated ground state and the transition state in the region of the R1 side chain.

Where the transition-state analog complexes differ most from the β -lactam acylated ground-state complexes is in the region of the tetrahedral center. In moving from the

planar ester center to the tetrahedral boronic acid, a hydrogen bond is gained between the O2 hydroxyl of the boronic acid and the hydroxyl of Tyr150. The O2, which appears to represent the position of the deacylating water in the high-energy intermediate [13], hydrogen bonds with Wat402. This water is conserved in native [12], acyl-enzyme [6], and transition-state analog structures [13], and it may identify the region from where the deacylating water attacks the acyl-adduct [6]. The O1 atom of the boronic acid, which represents the position of what was the lactam carbonyl oxygen in the acyl-enzyme intermediate [6], moves to pick up a hydrogen bond with the backbone oxygen of Ala318 in the tetrahedral adduct. This may be consistent with the status of this oxygen as a hydroxyl in the high-energy intermediate [12,13]. The overall picture that emerges is that, in moving from an acylated ground state to a transition-state analog complex, structural change is largely localized to the transition from a planar to a tetrahedral center in the ligand itself.

Once very effective, third-generation cephalosporins such as ceftazidime and cefotaxime have become largely useless against hospital pathogens such as *E. cloacae* because of the hyper-production of Group I β -lactamases. Given the high affinity of compounds **10** and **15** in enzyme assays, it seemed worthwhile to investigate their ability to reverse this resistance. Both inhibitors were synergistic when used in combination with the widely used third-generation cephalosporins ceftazidime (Fig. 6) and cefotaxime (Table 5). At high concentrations of **15**, the MIC values of these antibiotics were reduced by two orders of magnitude, close to the levels of non-resistant strains. The synergistic effect is perhaps shown most compellingly in the disk diffusion assays (Fig. 6). Against non-resistant *E. cloacae*, compounds **10** and **15** had no obvious effect, whereas against resistant strains of the same bacteria, these compounds showed an unmistakable synergy. Both inhibitors were also active against an isolate of *S. aureus* expressing a Group II β -lactamase, although efficacies were lower. The ability of **10** and **15** to reverse β -lactamase-based resistance, especially against the nosocomial pathogen *E. cloacae*, suggests that these compounds may be useful leads for the design of new agents to reverse bacterial resistance to β -lactams.

The X-ray crystal structures of AmpC with **9** and **11** may guide further inhibitor design. In the complex of **9** with AmpC, non-polar complementarity is achieved through interactions with residues Leu119, Leu293, and Ala318. The methyl group of the isoxazole ring of **9** forms van der Waals interactions with the Tyr221. The function of this conserved residue is unknown, but it often forms aromatic polar or stacking interactions with substrates [6] and inhibitors [6,13]. In both complexes, the R1 side chains only fill part of the enzyme cleft, leaving uncomplemented polar residues such as Asp123, Arg204, and Ser212. Interactions with some of these residues may help explain the increased affinity of **15**, which is the

most polar and the most active of the compounds tested. Intriguingly, Ser212 is just proximal to a site of a tandem insertion in a related Group I β -lactamase that leads to a mutant enzyme resistant to ceftazidime [26], the β -lactam analog of **15**. It may be possible to improve polar complementarity in this series to increase inhibition and specificity.

4. Significance

Penicillins and cephalosporins have had an enormous impact on human health. Unfortunately, the efficacy of these antibiotics is threatened by the emergence of β -lactamases. To understand how β -lactamases recognize β -lactam substrates and β -lactam inhibitors, it would be helpful to know what their binding energies are, but these have been difficult to measure because β -lactams form covalent adducts with β -lactamases. The reversible binding of the transition-state analog acylglycineboronic acids allows us to begin to dissect the energetic bases for recognition of the ubiquitous R1 side chains of β -lactam antibiotics by β -lactamases. We observe little relationship between affinity and whether the R1 side chain derives from a β -lactam substrate or a β -lactam inhibitor of the β -lactamase. Notwithstanding this, some R1 side chains bind tightly to β -lactamases, leading to inhibitors with low K_i values for these enzymes. These and related analogs are accessible synthetically and may provide useful tools for studying recognition and mechanism in β -lactamases. Several of the compounds are highly active and selective, and they reverse resistance to β -lactam antibiotics in pathogenic bacteria in cell culture. Coupling interaction energies with structure and synthesis may guide the design of anti-resistance agents in this series.

5. Materials and methods

5.1. Synthesis and analysis

^1H - and ^{13}C -NMR spectra were recorded on a Bruker DPX-200 MHz spectrometer and a Bruker-AMX-400 MHz spec-

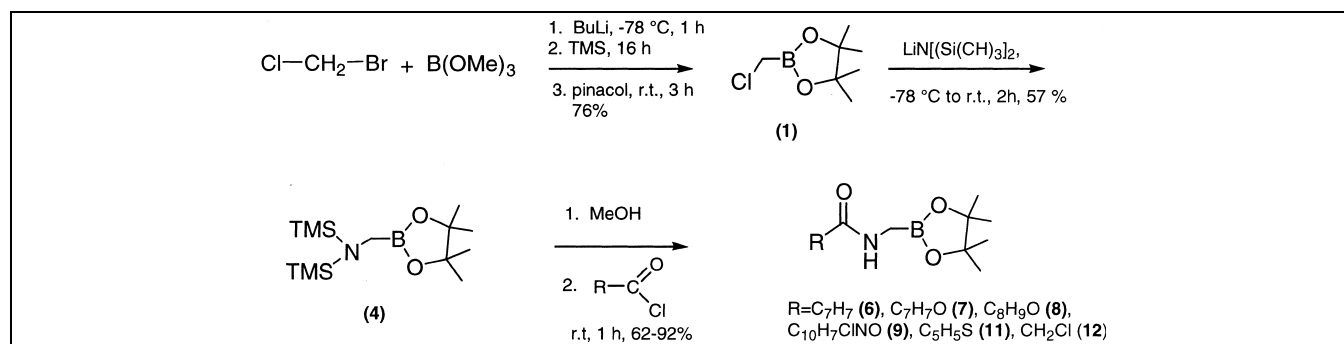
tively: chemical shifts are reported in δ values from TMS as internal standard (s singlet, d doublet, t triplet, br broad). Coupling constants (J) are given in Hz. Mass spectra were performed on a Finnigan MAT-SSQ 710A mass spectrometer and a Hewlett Packard 5872 (EI, 70 eV) mass spectrometer. Elemental analyses were determined with a Carlo Erba Elemental Analyzer mod. 1106; elemental analyses for the compounds were within $\pm 0.5\%$ of the theoretical values. IR spectra were recorded with a Perkin Elmer 1600 series FTIR; IR signals reported refer to C–O amide stretching and N–H amide stretching respectively. Solvents were dried and distilled before use; glassware was dried at 110°C for 40 min. All reactions were conducted under inert atmosphere unless otherwise specified. The common synthetic procedure is presented in Scheme 1.

5.1.1. Pinacol chloromethaneboronate (**1**) [27]

Butyl lithium in hexane (2.5 M, 9.2 ml, 23 mmol) was added dropwise to a stirred solution of bromochloromethane (1.5 ml, 23 mmol) and tri-*tert*-butylborate (2.3 ml, 21 mmol) in anhydrous THF (25 ml) at -78°C under nitrogen flow; the resulting mixture was allowed to react for 1 h. Thereafter, the reaction was quenched at -78°C with trimethylsilyl chloride (3.2 ml, 25.2 mmol), and the temperature gradually raised to room temperature (RT). After 16 h, a solution of pinacol (2.7 g, 23 mmol) in ethyl ether (10 ml) was added dropwise, and the mixture was stirred for an additional 3 h. The solution was diluted with water (20 ml) and ethyl ether (10 ml), and the aqueous phase was extracted with ethyl ether (3×10 ml). The combined organic phases were washed with brine and dried (MgSO_4). After removal of the solvent under reduced pressure, the oily residue was distilled in vacuo (bp $55\text{--}56^\circ\text{C}/2$ mm Hg) to yield **1** (3.08 g, 76%) as a colorless oil. ^1H -NMR (CDCl_3): δ 1.31 (12H, s, CH_3), 2.97 (2H, s, CH_2); ^{13}C -NMR (CDCl_3): δ 25.4, 85.3; MS, m/z : 178–176 (M^+), 163–161 (base peak), 145, 136–134, 120–118, 105–103, 85, 59, 43.

5.1.2. Pinacol *N,N'*-diformamidomethaneboronate (**2**) [28]

A solution of **1** (836 mg, 4.73 mmol) in anhydrous CH_3CN (2 ml) was added to a solution of sodium diformylamide (540 mg, 5.68 mmol) in anhydrous CH_3CN (2 ml) and the mixture stirred for 3 h at 80°C . The white precipitate (NaCl) was centrifuged off, the supernatant concentrated, and the residue distilled under reduced pressure to give **2** as a clear dense oil (735 mg, 73%), bp



Scheme 1. General scheme of synthesis of acylglycineboronic acids. See Section 4 for synthesis of boronic acids with other side chains.

83°C/1.5×10⁻² mm Hg. ¹H-NMR (CDCl₃): δ 1.25 (12H, s, CH₃), 3.19 (2H, s, CH₂), 8.86 (2H, s, COH); MS, *m/z*: 213 (M⁺), 198, 183, 155 (base peak), 114, 126, 97, 86.

5.1.3. Pinacol formamidomethaneboronate (3) [28]

Compound **2** (233 mg, 1.09 mmol) was dissolved in anhydrous methanol (1.2 ml) and stirred at RT for 1 h, until a GLC analysis showed disappearance of the starting material. The solution was concentrated in vacuo and triturated with CH₂Cl₂. The viscous oily residue crystallized overnight at 4°C to give **3** (200 mg, 99%) as a white solid, mp 55–56°C. IR (KBr) 1629, 3375 cm⁻¹; ¹H-NMR (CDCl₃): δ 1.32 (12H, s, CH₃), 2.93 (2H, d, *J* 4.5, CH₂), 5.70 (1H, br, NH), 8.20 (1H, s, CHO); ¹³C-NMR (DMSO): δ 24.7, 82.3, 162.2; MS, *m/z*: 185 (M⁺), 170, 154, 127 (base peak), 86, 70, 59, 43.

5.1.4. Pinacol bis-(trimethylsilyl)-aminomethaneboronate (4)

According to the procedure described [29], lithium hexamethyldisilazane in THF (1.0 M, 4.6 ml, 4.6 mmol) was added dropwise to a solution of **1** (800 mg, 4.6 mmol) in anhydrous ethyl ether (6 ml) cooled at -78°C under nitrogen. After stirring for 10 min at -78°C, the cooling bath was removed and the solution stirred for 2 h at RT. The precipitate (LiCl) was centrifuged, the supernatant concentrated under reduced pressure, and the oily residue was distilled under reduced pressure (bp 80–81°C/1 mm Hg) to give **4** (780 mg, 57%) as a colorless oil. ¹H-NMR (CDCl₃): δ 0.10 (18H, s, SiCH₃), 1.26 (12H, s, CH₃), 2.47 (2H, s, CH₂); MS, *m/z*: 301 (M⁺), 286, 228, 186 (base peak), 170, 112, 73, 59.

5.1.5. Pinacol acetamidomethaneboronate (5)

According to the procedure described [30], acetic acid (36.4 μl, 0.63 mmol) and acetic anhydride (165 μl, 1.75 mmol) were added at -10°C to a solution of **4** (150 mg, 0.5 mmol) in anhydrous Et₂O (3 ml) under inert atmosphere. After 1.5 h the solvent was evaporated in vacuo, and the residue crystallized from Et₂O/pentane to give **5** (60 mg, 60%) as a white solid, mp 108°C. IR (KBr) 1619, 3370 cm⁻¹; ¹H-NMR (CDCl₃): δ 1.26 (12H, s, CH₃), 2.07 (3H, s, COCH₃), 2.56 (2H, d, *J* 4.4, CH₂), 6.97 (1H, br, NH); ¹³C-NMR (DMSO): δ 24.2, 25.1, 79.3, 174.3; MS, *m/z*⁺: 199 (M⁺), 184, 169, 141, 140 (base peak), 100, 99, 84, 83, 74, 55.

5.1.6. Reaction of pinacol bis-(trimethylsilyl)-aminomethaneboronate (4) with acyl chlorides: general procedure [31]

A solution of anhydrous methanol in THF (1 mmol, 2.5 M) was added at -10°C to a solution of **4** (1 mmol) in THF under nitrogen. The cooling bath was removed, and the reaction mixture was stirred for 1 h at RT. The reaction mixture was once again cooled to -10°C. A solution of the acyl derivative (1 mmol) in THF was slowly added and allowed to react for the reported time whereupon a GLC analysis indicated total disappearance of **4**. The solvent was evaporated in vacuo and the residue purified by crystallization.

5.1.7. Pinacol phenylacetamidomethaneboronate (6)

Phenylacetylchloride was allowed to react with **4** for 1 h. The

solvent was evaporated and the viscous oily residue crystallized from hexane to give **6** (91% yield) as a pale yellow solid, mp 114°C. IR (KBr) 1615, 3169 cm⁻¹; ¹H-NMR (CDCl₃): δ 1.27 (12H, s, CH₃), 2.59 (2H, d, *J* 2.6, BCH₂), 3.68 (2H, s, PhCH₂), 6.97 (1H, br, NH), 7.24–7.44 (5H, m, aromatic); ¹³C-NMR (DMSO): δ 24.9, 38.4, 80.4, 126.8, 128.4, 128.9, 134.7, 174.0; MS, *m/z*: 275 (M⁺), 260, 217, 176, 160, 142, 91 (base peak), 83.

5.1.8. Pinacol phenoxyacetamidomethaneboronate (7)

After 1 h at RT, the solvent was evaporated and the residue crystallized from pentane to yield **7** (80%) as a white solid, mp 60°C. IR (KBr) 1630, 3454 cm⁻¹; ¹H-NMR (CDCl₃): δ 1.31 (12H, s, CH₃), 2.92 (2H, d, *J* 4.5, BCH₂), 4.55 (2H, s, OCH₂), 6.77 (1H, br, NH), 6.92–7.10 (3H, m, aromatic), 7.30–7.40 (2H, m, aromatic); ¹³C-NMR (DMSO): δ 24.7, 66.1, 82.3, 114.8, 121.2, 129.4, 157.6, 169.0; MS, *m/z*: 291 (M⁺), 276, 233 (base peak), 176, 98, 94, 77.

5.1.9. Pinacol [(2-phenoxypropanoyl)amino]methaneboronate (8)

After 1 h at RT, the solvent was evaporated to afford a white solid residue which was triturated with *n*-pentane to afford **8** (89%), mp 78°C. IR (KBr) 1621, 3186; ¹H-NMR (CDCl₃): δ 1.28 (12H, s, CCH₃), 1.61 (3H, d, *J* 6.8, CHCH₃), 2.83 (2H, d, *J* 4.5, CH₂), 4.73 (1H, q, *J* 6.8, CHCH₃), 6.65 (1H, br, NH), 6.91–7.08 (3H, m, aromatic), 7.27–7.38 (2H, m, aromatic); ¹³C-NMR (DMSO): δ 18.6, 24.6, 73.0, 82.4, 115.4, 121.1, 129.4, 157.1, 172.3; MS, *m/z*: 305 (M⁺), 290, 247 (base peak), 184, 121, 112, 83, 77.

5.1.10. Pinacol [(3-(2-chlorophenyl)-5-methyl-4-isoxazolyl)carbonyl] amino] methaneboronate (9)

After 1 h at RT, the solvent was evaporated and the residue crystallized from pentane to afford **9** (92%) as white crystalline solid, mp 91°C. IR (KBr) 1622, 3060; ¹H-NMR (CDCl₃): δ 1.21 (12H, s, CH₃), 2.74 (2H, d, *J* 3.8, CH₂), 2.81 (3H, s, CH₃), 5.59 (1H, br, NH), 7.40–7.51 (4H, m, aromatic); ¹³C-NMR (DMSO): δ 12.2, 24.7, 82.0, 111.8, 127.1, 127.4, 129.6, 131.4, 131.6, 132.6, 159.5, 161.9, 170.5; MS, *m/z*: 377 (M⁺), 341 (base peak), 318, 241, 215, 178, 111, 83.

5.1.11. Pinacol [(2-ethoxy-1-naphthoyl)amino]methaneboronic acid (10)

After 16 h at RT, solvent was removed affording a viscous residue, which was purified by silica column chromatography (elution: ethyl ether/ethyl acetate 1:1 v/v and then methanol) to give the free boronic acid **10** (57%) as a white solid, mp 150°C (dec). IR (KBr) 1630, 3250; ¹H-NMR (DMSO): δ 1.32 (3H, t, *J* 6.7, CH₃), 2.80 (2H, d, *J* 4.9, BCH₂), 4.20 (2H, d, *J* 6.7, OCH₂), 7.20–8.00 (9H, m, aromatic, NH, OH); ¹³C-NMR (DMSO): δ 14.9, 64.8, 64.9, 115.4, 122.5, 123.7, 124.5, 126.6, 127.7, 128.2, 129.8, 131.1, 152.2, 166.5; MS, *m/z*: 273 (M⁺), 229, 199, 171, 170, 155, 142, 127, 115 (base peak), 89, 88.

5.1.12. Pinacol α-thienylacetamidomethaneboronate (11)

After 1 h at RT, the solvent was removed and the residue

crystallized from ethyl ether/pentane yielding **7** (62%) as a white solid, mp 86–87°C. IR (KBr) 1619, 3169; $^1\text{H-NMR}$ (CDCl_3): δ 1.28 (12H, s, CH_3), 2.66 (2H, d, J 3.1, BCH_2), 3.87 (2H, s, ArCH_2), 6.10 (1H, br, NH), 6.97–7.03 (2H, m, aromatic), 7.28 (1H, dd, J 5.0, 1.5, S-CH); $^{13}\text{C-NMR}$ (DMSO): δ 24.8, 33.6, 81.3, 125.2, 126.4, 126.6, 136.2, 172.0; MS, m/z : 281 (M^+), 266, 223, 182, 166, 142, 97 (base peak), 83, 55.

5.1.13. Pinacol chloroacetamidomethaneboronate (**12**)

After 1.5 h at RT, the solvent was evaporated in vacuo affording **12** as a clear viscous oil (100%), which was used without further purification. $^1\text{H-NMR}$ (CDCl_3): δ 1.31 (12H, s, CH_3), 2.90 (2H, d, J 4.4, BCH_2), 4.09 (2H, s, CH_2Cl), 6.75 (1H, br, NH). $^{13}\text{C-NMR}$ (CDCl_3): δ 25.5, 43.1, 84.9, 167.6. MS, m/z : 235–233 (M^+), 220–218, 198, 177–175, 136–134, 119–117 (base peak), 98, 83, 55.

5.1.14. Pinacol (4-pyridil)thioacetamidomethaneboronate hydrochloride (**13**)

A solution of 4-mercaptopyridine (31 mg, 0.28 mmol) in anhydrous DMF (0.5 ml) was added under vigorous stirring to a solution of **12** (66 mg, 0.28 mmol) in anhydrous DMF (2 ml). After 3.5 h at 100°C, the solvent was evaporated under reduced pressure. The residue was crystallized from ethyl ether/pentane to give **13** as a white crystalline solid (90%), mp 186°C dec. IR (KBr) 1665, 3283 and 2550 ($\text{N}^+\text{-H}$ stretching); $^1\text{H-NMR}$ (DMSO): δ 1.16 (12H, s, CH_3), 2.52 (2H, d, J 4.3, BCH_2), 4.08 (2H, s, SCH_2), 7.85 (2H, dd, J 7.0, 1.4, $\text{H}(3)$, $\text{H}(5)$ aromatic), 8.52 (1H, br, NH), 8.62 (2H, dd, J 7.0, 1.2, $\text{H}(2)$, $\text{H}(6)$ aromatic); $^{13}\text{C-NMR}$ (DMSO): δ 24.6, 33.1, 82.8, 122.3, 140.4, 160.8, 167.0; MS, m/z : 308 (M^+), 293, 250, 209, 198, 152, 140, 125 (base peak), 111, 98, 83.

5.1.15. Pinacol [[2-amino- α -[1-(*tert*-butoxycarbonyl)-1-methylethoxyimino]-4-thiazoleacetyl]amino]methaneboronate (**14**)

Triethylamine (184 μl , 1.32 mmol) and isobutylchloroformate (171 μl , 1.32 mmol) were added to a solution of (*Z*)-2-amino- α -[1-(*tert*-butoxycarbonyl)-1-methylethoxyimino]-4-thiazoleacetic acid (438 mg, 1.32 mmol) in anhydrous THF (30 ml) at 0°C and allowed to react under inert atmosphere for 40 min. A solution of **4** (400 mg, 1.32 mmol) in anhydrous THF (4 ml), previously treated with anhydrous methanol (1.32 mmol) was added at the same temperature. After 20 min the temperature was raised to RT and the mixture allowed to react for 1 h. The white precipitate (ammonium chloride) was centrifuged, and the supernatant was evaporated under reduced pressure. The residue was crystallized from CH_2Cl_2 /pentane to give **14** as a white crystalline solid (80%), mp 188–190°C dec. IR (KBr) 1630, 1724, 3322; $^1\text{H-NMR}$ (CDCl_3): δ 1.32 (12H, s, CH_3), 1.47 (9H, s, $\text{C}(\text{CH}_3)_3$), 1.57 (6H, s, CH_3CCO), 1.81 (2H, br, NH_2), 3.00 (2H, d, J 4.4, CH_2NH), 6.98 (1H, t J 4.4, NH), 7.08 (1H, s, aromatic); $^{13}\text{C-NMR}$ (CDCl_3): δ 24.4, 25.6, 28.8, 82.6, 83.5, 85.0, 112.0, 143.3, 149.6, 163.7, 170.2, 174.5; MS, m/z : 468 (M^+), 453, 410, 367, 354, 309, 285, 251, 226, 209, 184, 142, 126 (base peak), 98, 83, 59.

5.1.16. Pinacol [[2-amino- α -(1-carboxy-1-methylethoxyimino)-4-thiazoleacetyl] amino]methaneboronate trifluoroacetic salt (**15**)

Compound **14** (200 mg, 0.43 mmol) was dissolved in trifluoroacetic acid (2.5 ml). After 50 min, the excess was evaporated under reduced pressure to give a dense oil which was crystallized from CH_2Cl_2 /*n*-hexane to afford a yellowish crystalline solid (80%), mp 161°C (dec). IR: 1661, 3286. $^1\text{H-NMR}$ (CDCl_3): δ 1.32 (12H, s, CH_3), 1.69 (6H, s, CH_3CCO), 2.99 (2H, d, J 4.3, CH_2), 5.76 (3H, b, NH_3^+), 7.31 (1H, s, aromatic), 7.92 (1H, t, J 4.3, NH), 8.24 (1H, b, COOH). $^{13}\text{C-NMR}$ (CDCl_3): 24.2, 25.4, 85.1, 85.8, 110.9, 133.4, 142.2, 160.1, 170.9, 176.3. MS, m/z : 412 (M^+), 397, 354, 310, 295, 268, 252, 229, 226, 221, 198, 185, 153, 129, 125, 103, 98 (base peak), 83, 69, 59.

5.2. Enzyme purification

AmpC from *Escherichia coli* was expressed and purified to homogeneity as described [12]. The TEM-1 gene was amplified from pBR322 by PCR and expressed from a pAlterEx II plasmid (Promega, Madison, WI, USA) from transformed *E. coli* JM109 cells. TEM-1 was expressed and purified using a procedure modified from Vanhove et al. [32]; a full description will be published elsewhere.

5.3. Enzyme inhibition assays

The pinacol esters of the acylglycineboronic acids were hydrolyzed to the free acids by dissolving them in 50 mM phosphate buffer at pH 7.0 [33] at a concentration of 10 mM; more dilute stocks (1 mM to 100 μM) were subsequently prepared as necessary. Kinetic measurements with AmpC were performed using cephalothin as a substrate [11]. Reactions were initiated by the addition of 1.5 nM enzyme. No incubation effect was detected for any compound, consistent with earlier studies [11,25]. IC_{50} values were determined at 100 μM substrate concentration.

TEM-1 enzyme assays used 100 μM furylacryloylamidopenicillanic acid as substrate, monitoring absorbance changes at 340 nm on an HP8453 spectrophotometer. Reactions were initiated with addition of 0.3 nM enzyme, using the same buffer as in the AmpC assays.

The K_i values for compounds **3–14** were obtained by comparison of progress curves in the presence and absence of inhibitor [25]. Sufficient inhibitor was used to give at least 50% inhibition. This method correlates well with full K_i analysis through coupled substrate and inhibitor concentration variation [11]. For compound **9**, a K_i of 170 ± 10 nM, consistent with the value of 160 nM determined by progress curve analysis, was also determined by Lineweaver–Burk analysis of multiple substrate and inhibitor concentrations (data not shown).

The selectivity of compounds **3** and **15** for β -lactamases was determined by measuring their activity against α -chymotrypsin (bovine pancreatic), β -trypsin (bovine pancreatic), and elastase (porcine pancreatic), all from Sigma (St. Louis, MO, USA). Substrates for α -chymotrypsin (*N*-benzoyl-L-tyrosine ethyl ester, BTEE) and β -trypsin (*N*-benzoyl-L-arginine ethyl ester, BAEE)

were also purchased from Sigma. The elastase substrate used (elastase substrate 1, MeOSuc-Ala-Ala-Pro-Val-pNA) was purchased from Calbiochem (San Diego, CA, USA). Substrates were diluted from 10 mM DMSO stock solutions, and all reactions were performed in 50 mM potassium phosphate buffer, pH 7.0, 25°C. For α -chymotrypsin, 140 μ M of BTEE was used, the reactions were initiated by addition of 5 μ l of a 0.1 mg/ml enzyme stock solution, and monitored at 260 nm. For β -trypsin, 200 μ M of BAEE was used, the reactions were initiated by the addition of 5 μ l of a 0.2 mg/ml enzyme stock solution, and monitored at 260 nm. For elastase, 640 μ M of elastase substrate was used, the reactions were initiated by the addition of 30 μ l of a 0.2 mg/ml enzyme stock solution, and monitored at 385 nm. Initial rate fits to the absorbance data for the first 150 s of each reaction were used to determine reaction velocities.

5.4. Crystal growth and structure determination

Co-crystals of **9** and **11** were grown by vapor diffusion in hanging drops equilibrated over 1.7 M potassium phosphate buffer (pH 8.7) using microseeding techniques. The initial concentration of protein in the drop was 95 μ M, and the concentrations of each inhibitor were 586 μ M. The inhibitors were added to the crystallization drop in a 2% DMSO, 1.7 M potassium phosphate buffer (pH 8.7) solution. Crystals appeared within 3–5 days after equilibration at 23°C.

Data were collected on the DND-CAT beam line (5IDB) of the Advanced Photon Source at Argonne National Lab at 100 K using a 162 mm Mar CCD detector. Prior to data collection, crystals were immersed in a cryoprotectant solution of 20% sucrose, 1.7 M potassium phosphate, pH 8.7, for about 20 s, then flash-cooled in liquid nitrogen. Each data set was measured from a single crystal.

Reflections were indexed, integrated, and scaled using the HKL program suite [34] (Table 3). The space group was C2, with two AmpC molecules in the asymmetric unit. Each AmpC molecule contained 358 residues. The structure was determined by molecular replacement using an AmpC/boronic acid complexed structure [13], with inhibitor and water molecules removed, as the initial phasing model. The model was refined using the maximum likelihood target in CNS and included a bulk solvent correction [35]. Sigma A-weighted electron density maps were calculated using CNS, and manual rebuilding was done in the program O [36]. The inhibitor was built into the observed difference density in each active site of the asymmetric unit, and the structure of the complex was further refined using CNS (Table 3). All atoms of inhibitor **9** were refined with an occupancy of 1.0. All atoms of inhibitor **11** were refined with an occupancy of 1.0, except for atoms of the thiophene ring (C9, C10, C11 and S1) which were refined with an occupancy of 0.5 for each of the two possible conformations.

5.5. Microbiology

Compounds **10** and **15** were tested for synergy with β -lactams against pathogenic bacteria that are sensitive to β -lactams and to

pathogenic bacteria that are resistant to β -lactams through production of either Group I or Group II β -lactamases. Bacterial strains tested included: *E. cloacae* EB5 (β -lactamase negative), *E. cloacae* 265A (Group I β -lactamase hyper-producer), and *S. aureus* V41 (Group II β -lactamase producer). MIC values were determined with Mueller–Hinton Broth II using the microdilution method according to NCCLS guidelines [37]. The β -lactams cefotaxime and ceftazidime were used with *E. cloacae*, and amoxicillin was used with *S. aureus*. Checkerboard assays were performed to study the synergistic effects.

Disk diffusion plate assays were performed as follows. *E. cloacae* EB5 and *E. cloacae* 265A were each grown to log-phase and then diluted in TY broth to a turbidity equivalent to McFarland 1. The cultures were further diluted 100-fold into melted TY agar medium and allowed to solidify in Falcon 150 \times 25 mm plates. The plates were then spotted with ceftazidime (25 μ g per disk for the EB5 plate and 50 μ g per disk for the 265A plate; upper disks) and 100 μ g of **15** (lower disks on the left) and 100 μ g of **10** (lower disks on the right). After overnight incubation at 35 °C, the zones of inhibition were imaged.

Acknowledgements

This work was supported by NIH GM59957 and NSF MCB-9734484 (to B.K.S.). E.C. thanks the Italian University Ministry of Scientific and Technological Research for financial support and Professor Irene Moretti for mentoring. R.A.P. was partly supported by NIH Training Grant T32 ES07284. We thank P. Focia and G. Minasov for advice with crystallographic methods, and D. Lorber, X. Wang, S. McGovern, and B. Beadle for reading this manuscript. The DuPont-Northwestern-Dow Collaborative Access Team at the APS is supported by E.I. DuPont de Nemours and Co., the Dow Chemical Company, the National Science Foundation, and the State of Illinois.

References

- [1] H.C. Neu, The crisis in antibiotic resistance, *Science* 257 (1992) 1064–1073.
- [2] D. Monnaie, R. Viriden, J.M. Frere, A rapid-kinetic study of the class C β -lactamase of *Enterobacter cloacae* 908R, *FEBS Lett.* 306 (1992) 108–112.
- [3] A. Matagne, A.M. Misselyn-Bauduin, B. Joris, T. Erpicum, B. Granier, J.M. Frere, The diversity of the catalytic properties of class A β -lactamases, *Biochem. J.* 265 (1990) 131–146.
- [4] M. Galleni, J. Lamotte-Brasseur, X. Raquet, A. Dubus, D. Monnaie, J.R. Knox, J.M. Frere, The enigmatic catalytic mechanism of active-site serine β -lactamases, *Biochem. Pharmacol.* 49 (1995) 1171–1178.
- [5] L. Maveyraud, L. Mourey, L.P. Kotra, J.D. Pedelacq, V. Guillet, S. Mobashery, J.P. Samama, Structural basis for clinical longevity of carbapenem antibiotics in the face of challenge by the common class A β -lactamases from the antibiotic-resistant bacteria, *J. Am. Chem. Soc.* 120 (1998) 9748–9752.
- [6] A. Patera, L.C. Blaszcak, B.K. Shoichet, Crystal structures of substrate and inhibitor complexes with AmpC β -lactamase: possible im-

- plications for substrate-assisted catalysis, *J. Am. Chem. Soc.* (2000) in press.
- [7] B.M. Beadle, S.L. McGovern, A. Patera, B.K. Shoichet, Functional analyses of AmpC β -lactamase through differential stability, *Protein Sci.* 8 (1999) 1816–1824.
- [8] T. Beesley, N. Gascoyne, V. Knott-Hunziker, S. Petursson, S.G. Waley, B. Jaurin, T. Grundstrom, The inhibition of class C β -lactamases by boronic acids, *Biochem. J.* 209 (1983) 229–233.
- [9] I.E. Crompton, B.K. Cuthbert, G. Lowe, S.G. Waley, β -Lactamase inhibitors. The inhibition of serine β -lactamases by specific boronic acids, *Biochem. J.* 251 (1988) 453–459.
- [10] N.C. Strynadka, R. Martin, S.E. Jensen, M. Gold, J.B. Jones, Structure-based design of a potent transition state analogue for TEM-1 β -lactamase, *Nature Struct. Biol.* 3 (1996) 688–695.
- [11] G.S. Weston, J. Blazquez, F. Baquero, B.K. Shoichet, Structure-based enhancement of boronic acid-based inhibitors of AmpC β -lactamase, *J. Med. Chem.* 41 (1998) 4577–4586.
- [12] K.C. Usher, L.C. Blaszcak, G.S. Weston, B.K. Shoichet, S.J. Remington, Three-dimensional structure of AmpC β -lactamase from *Escherichia coli* bound to a transition-state analogue: Possible implications for the oxyanion hypothesis and for inhibitor design, *Biochemistry* 37 (1998) 16082–16092.
- [13] R.A. Powers, J. Blazquez, G.S. Weston, M.I. Morosini, F. Baquero, B.K. Shoichet, The complexed structure and antimicrobial activity of a non- β -lactam inhibitor of AmpC β -lactamase, *Protein Sci.* 8 (1999) 2330–2337.
- [14] S. Ness, R. Martin, A.M. Kindler, M. Paetzel, M. Gold, S.E. Jensen, J.B. Jones, N.C. Strynadka, Structure-based design guides the improved efficacy of deacylation transition state analogue inhibitors of TEM-1 β -lactamase, *Biochemistry* 39 (2000) 5312–5321.
- [15] R.A. Laskowski, M.W. MacArthur, D.S. Moss, J.M. Thornton, PROCHECK: a program to check the stereochemical quality of protein structures, *J. Appl. Crystallogr.* 26 (1993) 283–291.
- [16] E. Lobkovsky, E.M. Billings, P.C. Moews, J. Rahil, R.F. Pratt, J.R. Knox, Crystallographic structure of a phosphonate derivative of the *Enterobacter cloacae* P99 cephalosporinase: mechanistic interpretation of a β -lactamase transition-state analog, *Biochemistry* 33 (1994) 6762–6772.
- [17] A. Dubus, P. Ledent, J. Lamotte-Brasseur, J.M. Frere, The roles of residues Tyr150, Glu272, and His314 in class C β -lactamases, *Proteins* 25 (1996) 473–485.
- [18] C. Oefner, A. D'Arcy, J.J. Daly, K. Gubernator, R.L. Charnas, I. Heinze, C. Hubschwerlen, F.K. Winkler, Refined crystal structure of β -lactamase from *Citrobacter freundii* indicates a mechanism for β -lactam hydrolysis, *Nature* 343 (1990) 284–288.
- [19] N.C. Strynadka, H. Adachi, S.E. Jensen, K. Johns, A. Sielecki, C. Betzel, K. Sutoh, M.N. James, Molecular structure of the acyl-enzyme intermediate in β -lactam hydrolysis at 1.7 Å resolution (see comments), *Nature* 359 (1992) 700–705.
- [20] C.A. Kettner, R. Bone, D.A. Agard, W.W. Bachovchin, Kinetic properties of the binding of α -lytic protease to peptide boronic acids, *Biochemistry* 27 (1988) 7682–7688.
- [21] C.C. Chen, J. Rahil, R.F. Pratt, O. Herzberg, Structure of a phosphonate-inhibited β -lactamase. An analog of the tetrahedral transition state/intermediate of β -lactam hydrolysis, *J. Mol. Biol.* 234 (1993) 165–178.
- [22] J. Osuna, H. Viadiu, A.L. Fink, X. Soberon, Substitution of Asp for Asn at position 132 in the active site of TEM β -lactamase. Activity toward different substrates and effects of neighboring residues, *J. Biol. Chem.* 270 (1995) 775–780.
- [23] A. Dubus, S. Normark, M. Kania, M.G. Page, Role of asparagine 152 in catalysis of β -lactam hydrolysis by *Escherichia coli* AmpC β -lactamase studied by site-directed mutagenesis, *Biochemistry* 34 (1995) 7757–7764.
- [24] L. Varetto, F. De Meester, D. Monnaie, J. Marchand-Brynaert, G. Dive, F. Jacob, J.M. Frere, The importance of the negative charge of β -lactam compounds in the interactions with active-site serine DD-peptidases and β -lactamases, *Biochem. J.* 278 (1991) 801–807.
- [25] S.G. Waley, A quick method for the determination of inhibition constants, *Biochem. J.* 205 (1982) 631–633.
- [26] G.V. Crichlow, A.P. Kuzin, M. Nukaga, K. Mayama, T. Sawai, J.R. Knox, Structure of the extended-spectrum class C β -lactamase of *Enterobacter cloacae* GC1, a natural mutant with a tandem tripeptide insertion, *Biochemistry* 38 (1999) 10256–10261.
- [27] A. Whiting, A convenient preparation of β -boronate carbonyl derivatives – evidence for the intervention of boronate 'ATE'-complexes in enolate alkylations, *Tetrahedron Lett.* 32 (1991) 1503–1506.
- [28] J.P.G. Versleijen, P.M. Faber, H.H. Bodewes, A.H. Braker, D. Vanleusen, A.M. Vanleusen, On the synthesis of boron-substituted methyl isocyanides – 2-isocyanomethyl-4,4,5,5-tetramethyl-1,3,2-dioxaborolane, *Tetrahedron Lett.* 36 (1995) 2109–2112.
- [29] C. Lebarbier, F. Carreaux, B. Carboni, Synthesis of a Boronic Acid Analogue of L-Orithine, *Synthesis*, Stuttgart, 1996, pp. 1371–1374.
- [30] D.S. Matteson, T.J. Michnick, R.D. Willett, C.D. Patterson, [(1R)-1-acetamido-3-(methylthio)propyl]boronic acid and the X-ray structure of its ethylene-glycol ester, *Organometallics* 8 (1989) 726–729.
- [31] D.S. Matteson, P.K. Jesthi, K.M. Sadhu, Synthesis and properties of pinanediol α -amido boronic esters, *Organometallics* 3 (1984) 1284–1288.
- [32] M. Vanhove, G. Guillaume, P. Ledent, J.H. Richards, R.H. Pain, J.M. Frere, Kinetic and thermodynamic consequences of the removal of the Cys-77–Cys-123 disulphide bond for the folding of TEM-1 β -lactamase, *Biochem. J.* 321 (1997) 413–417.
- [33] C.A. Kettner, A.B. Shenvi, Inhibition of the serine proteases leukocyte elastase, pancreatic elastase, cathepsin G, and chymotrypsin by peptide boronic acids, *J. Biol. Chem.* 259 (1984) 15106–15114.
- [34] Z. Otwinowski, W. Minor, Processing of X-ray diffraction data collected in oscillation mode, *Methods Enzymol.* 276 (1997) 307–326.
- [35] A.T. Brunger, P.D. Adams, G.M. Clore, W.L. DeLano, P. Gros, R.W. Grosse-Kunstleve, J.S. Jiang, J. Kuszewski, M. Nilges, N.S. Pannu, R.J. Read, L.M. Rice, T. Simonson, G.L. Warren, Crystallography and NMR system: A new software suite for macromolecular structure determination, *Acta Crystallogr. D Biol. Crystallogr.* 54 (1998) 905–921.
- [36] T.A. Jones, J.Y. Zou, S.W. Cowan, M.K. Kjeldgaard, Improved methods for building protein models in electron density maps and the location of errors in these models, *Acta Crystallogr. A* 47 (1991) 110–119.
- [37] National Committee for Clinical Laboratory Standards, Methods for dilution antimicrobial susceptibility tests for bacteria that grow aerobically. Approved Standard M7-A4, vol. 17, National Committee for Clinical Laboratory Standards, Villanova, PA, 1997.
- [38] C. Cambillau, A. Roussel, Turbo Frodo, Universite Aix-Marseille II, Marseille, 1997.
- [39] T.E. Ferrin, C.C. Huang, L.E. Jarvis, R. Langridge, The MIDAS display system, *J. Mol. Graph.* 6 (1988) 13–27.